

See discussions, stats, and author profiles for this publication at: <https://www.researchgate.net/publication/236131606>

^{31}P - ^{31}P spin-spin coupling constants for pnictogen homodimers

ARTICLE in CHEMICAL PHYSICS LETTERS · AUGUST 2011

Impact Factor: 1.9 · DOI: 10.1016/j.cplett.2011.07.043

CITATIONS

64

READS

61

4 AUTHORS, INCLUDING:



Ibon Alkorta

Spanish National Research Council

680 PUBLICATIONS 12,435 CITATIONS

SEE PROFILE



Goar Sánchez

University College Dublin

69 PUBLICATIONS 905 CITATIONS

SEE PROFILE

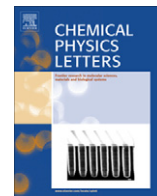


José Elguero

Spanish National Research Council

1,502 PUBLICATIONS 22,232 CITATIONS

SEE PROFILE



^{31}P – ^{31}P spin–spin coupling constants for pnictogen homodimers

Janet E. Del Bene^{a,*}, Ibon Alkorta^{b,*}, Goar Sanchez-Sanz^b, José Elguero^b

^a Department of Chemistry, Youngstown State University, Youngstown, OH 44555, USA

^b Instituto de Química Médica, CSIC, Juan de la Cierva, 3, E-28006 Madrid, Spain

ARTICLE INFO

Article history:

Received 4 June 2011

In final form 13 July 2011

Available online 20 July 2011

ABSTRACT

Ab initio calculations have been carried out in a systematic investigation of pnictogen homodimers $(\text{PH}_2\text{X})_2$, for $\text{X} = \text{F}, \text{OH}, \text{NC}, \text{NH}_2, \text{CCH}, \text{CN}, \text{CH}_3, \text{H}$, and BH_2 . Complex binding energies range from 7 to 34 kJ mol^{-1} , which is within the range observed for neutral hydrogen-bonded complexes. One-bond spin–spin coupling constants across the pnictogen interaction $^1J(\text{P}–\text{P})$ exhibit a quadratic dependence on the P–P distance, similar to the dependence of $^2J(\text{X}–\text{Y})$ on the X–Y distance for complexes with $\text{X}–\text{H} \cdots \text{Y}$ hydrogen bonds. Thus, computed values of $^1J(\text{P}–\text{P})$ could be used to extract P–P distances from experimentally measured coupling constants.

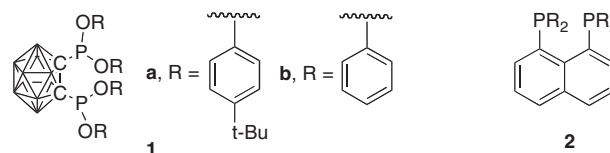
© 2011 Elsevier B.V. All rights reserved.

1. Introduction

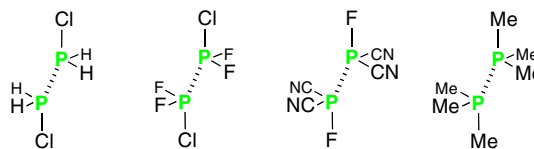
The number of known stabilizing intermolecular interactions is continuously increasing. These now include interactions between identical atoms such as $\text{H} \cdots \text{H}$ (di-hydrogen bonds), $\text{Br} \cdots \text{Br}$ (halogen bonds), $\text{S} \cdots \text{S}$ (chalcogen bonds) and $\text{P} \cdots \text{P}$ (pnictogen bonds). The same types of interactions can also be found between different atoms from the same group, such as $\text{Br} \cdots \text{Cl}$, $\text{S} \cdots \text{Se}$, and $\text{N} \cdots \text{P}$. These relatively new types of intermolecular interactions join the list of more traditional ones such as hydrogen bonds and lithium bonds, and present new challenges to both experimentalists and theorists to explain their fundamental nature, evaluate their properties, and utilize them in creative ways.

The P–P pnictogen bond is of special interest not only as a new type of intermolecular interaction, but also as one in which the bonded atoms may exhibit large values of spin–spin coupling constants even though they are not covalently bonded. For example, in 2009, Hey-Hawkins and co-workers measured an experimental ^{31}P – ^{31}P coupling constant of 105 Hz for molecule **1** (1,2-bis[bis(4-*tert*-butylphenoxy)phosphanyl]-*clos*-dicarbaborane(12)) [1]. Jackson et al. measured a four-bond coupling constant $^4J(\text{P}–\text{P})$ equal to 199 Hz for a diphosphine analogue of a proton sponge **2**, and suggested a significant through-space component for this P–P coupling [2]. Sundberg et al. [3] determined the X-ray structure of **1** with $\text{R} = \text{Ph}$, and found a $\text{P} \cdots \text{P}$ distance of 3.2225(12) Å, clearly less than the sum of the van der Waals radii of two P atoms, but longer than an intramolecular P–P bond. From natural bond orbital (NBO) analyses, they computed stabilization energies of about 8 and 13 kJ mol^{-1} for molecules **1a** and **1b**, which they attributed to a

charge-transfer interaction involving the lone pair orbital on one P to an antibonding P–C orbital on the other.



In a recent Letter, Hey-Hawkins and co-workers carried out a high-level theoretical study of the pnictogen P–P bond for a series of complexes, a few of which are illustrated below. They used the NBO, ELF and SAPT methods to analyze these complexes, and described the pnictogen bond as a new molecular linker [4]. Hey-Hawkins and co-workers also investigated an $\text{N} \cdots \text{P}$ pnictogen interaction in an aminoalkylferrocenyldichlorophosphane [5].



In a series of papers, we have investigated properties of complexes stabilized by various types of intermolecular interactions [6,7], including hydrogen bonds [8–10], dihydrogen bonds [11], halogen bonds [12,13], and lithium bonds [14,15], and have characterized these interactions in terms of associated spin–spin coupling constants. Given the very unique character of the pnictogen bond and the absence of both experimental and theoretical NMR data for pnictogen complexes, we decided to embark upon a systematic investigation of a series of homodimers derived from monosubstituted PH_3 molecules, represented as $(\text{PH}_2\text{X})_2$, for $\text{X} = \text{F}, \text{OH}, \text{NC}, \text{NH}_2, \text{CCH}, \text{CN}, \text{CH}_3, \text{H}$, and BH_2 . Our aim is to investigate their structures and binding energies, and to examine the extent to

* Corresponding authors. Fax: +1 330 941 1579 (J.E. Del Bene).

E-mail addresses: jedelbene@ysu.edu (J.E. Del Bene), ibon@iqm.csic.es (I. Alkorta).

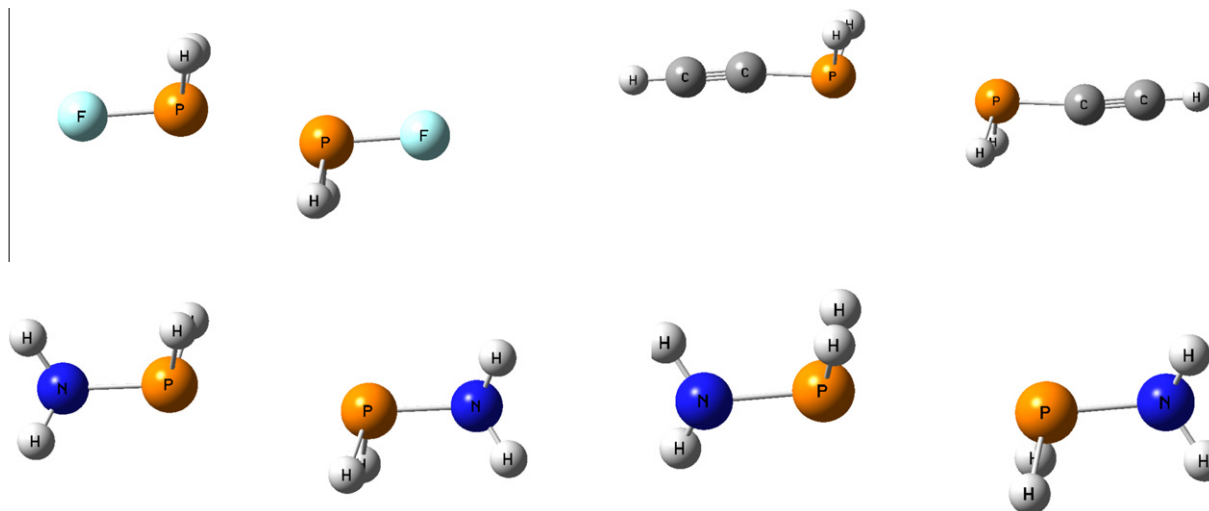


Figure 1. Homodimers $(\text{PH}_2\text{F})_2$, $[\text{PH}_2(\text{CCH})]_2$, and $[\text{PH}_2(\text{NH}_2)]_2$ C_2 and C_i structures.

which these complexes can be characterized by ^{31}P – ^{31}P spin–spin coupling constants. In this Letter we present the results of this investigation.

2. Computational details

The structures of the monomers PH_2F , $\text{PH}_2(\text{OH})$, $\text{PH}_2(\text{NC})$, $\text{PH}_2(\text{NH}_2)$, $\text{PH}_2(\text{CCH})$, $\text{PH}_2(\text{CN})$, $\text{PH}_2(\text{CH}_3)$, PH_3 , and $\text{PH}_2(\text{BH}_2)$ and of the homodimers $(\text{PH}_2\text{X})_2$ formed from these monomers were optimized at second-order Møller-Plesset perturbation theory (MP2) [16–19] with the aug'-cc-pVTZ basis set [20], which is the Dunning aug-cc-pVTZ basis [21,22] without diffuse function on H atoms. Frequency calculations were carried out to confirm that the optimized structures are local minima on their potential surfaces. The optimization and frequency calculations were carried out using GAUSSIAN-09 [23].

Electron densities have been analyzed using the atoms in molecules (AIM) methodology [24,25] with the AIM-PAC and AIM-ALL programs [26,27]. Electron density changes upon complex formation have been evaluated as the difference between the electron density of the complex and that of the isolated monomers at their geometry in the complex.

Indirect spin–spin coupling constants were computed using the equation-of-motion coupled cluster singles and doubles (EOM-CCSD) method in the CI (configuration interaction)-like approximation [28,29], with all electrons correlated. For these calculations, the Ahlrichs and co-workers [30] qzp basis set was placed on ^{13}C , ^{15}N , ^{17}O , and ^{19}F atoms, the qz2p basis set on ^{31}P , and a corresponding hybrid basis set on ^7B [31]. The Dunning cc-pVDZ basis [21,22] was placed on H atoms. Analogous to the designation of coupling constants across hydrogen bonds, we designate the P–P coupling constants across pnictogen bonds as $^1J(\text{P-P})$. These coupling constants were evaluated as a sum of four terms, namely, the paramagnetic spin-orbit (PSO), diamagnetic spin-orbit (DSO), Fermi-contact (FC), and spin-dipole (SD) [32]. The coupling constant calculations were carried out using ACES II [33] on the IBM 1350 cluster (Glenn) at the Ohio Supercomputer Center.

3. Results and discussion

3.1. Structures, binding energies, and bonding

The geometries of the pnictogen homodimers $(\text{PH}_2\text{X})_2$ are given in Table S1 of the Supplementary data, and representative

Table 1

MP2/aug'-cc-pVTZ P–P distances (R, Å), A–P–P angles (\angle , °) binding energies (ΔE , kJ mol $^{-1}$), and spin–spin coupling constants [$^1J(\text{P-P})$, Hz] for pnictogen homodimers.

Complex	R(P–P)	$\angle\text{A-P-P}^a$	ΔE	$^1J(\text{P-P})$
$(\text{PH}_2\text{F})_2$	2.471	163	33.97	998.6
$[\text{PH}_2(\text{OH})]_2$	2.851	169	20.55	644.0
$[\text{PH}_2(\text{NC})]_2$	3.040	168	13.76	640.3
$[\text{PH}_2(\text{NH}_2)]_2\text{-C}_2$	3.220	170	12.94	357.8
$[\text{PH}_2(\text{NH}_2)]_2\text{-C}_i$	3.221	170	13.04	358.3
$[\text{PH}_2(\text{CCH})]_2$	3.353	174	12.23	281.9
$[\text{PH}_2(\text{CN})]_2$	3.375	171	8.37	300.0
$[\text{PH}_2(\text{CH}_3)]_2$	3.481	178	8.88	160.9
$(\text{PH}_3)_2$	3.589	179	7.08	130.9
$[\text{PH}_2(\text{BH}_2)]_2$	3.744	174	7.04	46.0

^a Atom A is the atom of group X that is directly bonded to P.

complexes are illustrated in Figure 1. Equilibrium structures have C_{2h} symmetry, except for the two structures of $[\text{PH}_2(\text{NH}_2)]_2$, which have C_2 and C_i symmetry. One interesting structural feature of these complexes which is evident from Figure 1 is the nearly linear arrangement of atoms A–P···P–A, where A is the atom of the substituent X which is directly bonded to P. Table 1 presents the intermolecular P–P distances, A–P–P angles, and binding energies for these complexes.

The intermolecular P–P distances range from 2.471 to 3.744 Å. These distances are longer than the P–P bond distances of 2.224, 2.238, and 2.266 Å, respectively, for the optimized H_2P – PH_2 equilibrium C_2 structure, and optimized C_{2h} and C_{2v} structures, respectively. The binding energies of the homodimers lie between 7 and 34 kJ mol $^{-1}$, a range which is comparable to the binding energies of neutral hydrogen-bonded complexes. It is interesting to note that the most tightly-bound dimer is that in which the substituent X is electron-rich (F), while the weakest dimer has the electron-deficient BH_2 group as the substituent.

Table S2 of the Supplementary data provides values of the electron density, Laplacian, and energy density at P–P bond critical points (bcp's) obtained from the AIM analyses. The electron density at the bcp shows an exponential relationship with the interatomic distance similar to that described for hydrogen bonded systems [34], with a correlation coefficient of 0.999. The energy densities at the bcp indicate that the pnictogen bonds in the three most strongly bound complexes have some covalent character.

It is important to note that there is a significant electron-density overlap in the region between the two phosphorus atoms. Fig-

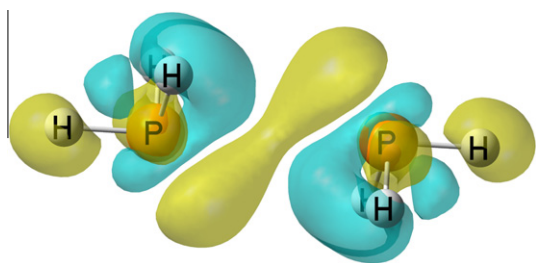


Figure 2. Electron density shifts for $(\text{PH}_3)_2$ at the ± 0.0001 au isosurface. Blue and yellow regions indicate regions of decreased and increased electron densities, respectively.

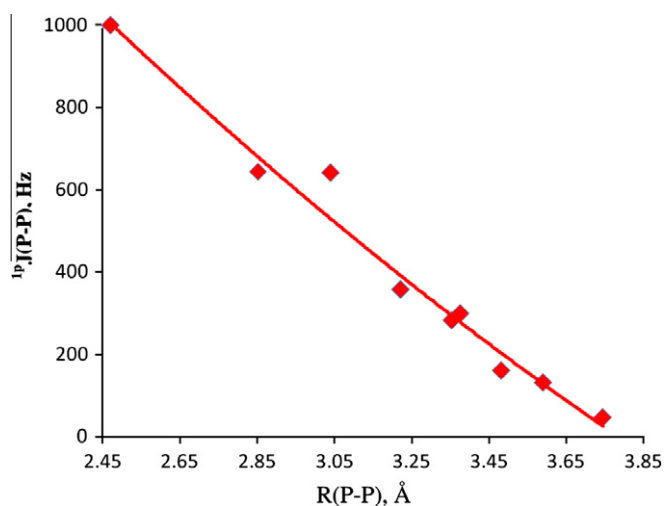


Figure 3. $^1pJ(\text{P-P})$ versus the P–P distance for pnictogen homodimers.

Figure 2 illustrates the increase in electron density in that region, and at the atoms which are aligned with the P–P bond. Electron density loss is experienced in the region near the two phosphorus nuclei, and by the out-of-plane H atoms. It is the build-up of charge in the region between the two P nuclei that results in the formation of the pnictogen bond.

3.2. Coupling constants

Table 1 also reports coupling constants $^1pJ(\text{P-P})$ for the pnictogen homodimers, and the components of $^1pJ(\text{P-P})$ are reported in Table S3 of the Supplementary data. These data show that the FC term is an excellent approximation to $^1pJ(\text{P-P})$. Thus, the P–P coupling constant depends on ground-state s electron densities and on s electron densities in excited states which couple to the ground state through the FC operator.

The data of Table 1 show that $^1pJ(\text{P-P})$ varies from 50 Hz for $[\text{PH}_2(\text{BH}_2)]_2$ to 1000 Hz for $(\text{PH}_2\text{F})_2$, thus illustrating the sensitivity of P–P coupling to the nature of X. An increase of this coupling constant upon substitution in PH_3 of an electron-withdrawing group is consistent with both experimental and computed EOM–CCSD data for the effect of fluoro-substitution on $^1J(\text{C-C})$ for benzene [35]. The decrease in $^1pJ(\text{P-P})$ upon substitution of the electron-donating BH_2 group is also consistent with previous findings concerning the effect of Li substitution on one-bond coupling constants in substituted borazine rings [36]. Figure 3 presents a plot of $^1pJ(\text{P-P})$ versus the P–P distance. $^1pJ(\text{P-P})$ increases quadratically as the intermolecular P–P distance decreases, with a correlation coefficient of 0.975. The large range of values of this coupling constant

Table 2

P–P distance (R, Å) and $^1J(\text{P-P})$ and its components (Hz) for P_2H_4 ^a.

Symmetry	R	PSO	FC	SD	$^1J(\text{P-P})$
C_{2h}	2.238	14.4	−44.7	47.9	17.7
C_2	2.224	8.2	−164.6	41.7	−114.7
C_{2v}	2.266	45.0	−230.1	52.8	−132.2

^a The DSO term is 0.1 Hz for each entry.

and the good correlation with distance imply that it would be possible to extract intermolecular P–P distances from the experimental values of $^1J(\text{P-P})$. The distance dependence of $^1pJ(\text{P-P})$ across the P–P pnictogen bond resembles the X–Y distance dependence of $^2hJ(\text{X-Y})$ across an X–H...Y hydrogen bond.

Finally, $^1pJ(\text{P-P})$ for the pnictogen complexes can be compared with $^1J(\text{P-P})$ for the P_2H_4 molecule. A previous study of one-bond coupling constants in molecules $\text{H}_m\text{X-YH}_n$ including $\text{H}_2\text{P-PH}_2$ found that $^1J(\text{X-Y})$ is extremely sensitive to rotation around the X–Y bond [37]. This can also be seen from the values of $^1J(\text{P-P})$ and its components in Table 2 for the equilibrium C_2 structure of P_2H_4 and for optimized C_{2v} and C_{2h} structures. For the C_{2h} structure, the largest contributions to $^1J(\text{P-P})$ comes from the positive SD term (48 Hz) and the negative FC term (−45 Hz). The PSO term makes a smaller positive contribution (14 Hz), with the result that $^1J(\text{P-P})$ is small (18 Hz) and positive. For the C_2 and C_{2v} structures, the FC term is dominant and negative, contributing −165 and −230 Hz, respectively, to total J values of −115 and −132 Hz, respectively. The PSO and SD terms make smaller, positive contributions. Thus, P–P coupling in the complexes across the pnictogen bond is dramatically different from P–P coupling in a molecule in which the two P atoms are covalently bonded.

4. Conclusions

Ab initio calculations have been carried out in a systematic investigation of pnictogen homodimers represented as $(\text{PH}_2\text{X})_2$, for X = F, OH, NC, NH_2 , CCH, CN, CH_3 , H, and BH_2 . The intermolecular distances in these complexes are shorter than the sum of the van der Waals radii of two P atoms, but longer than covalent P–P bonds. Complex binding energies lie in the same range as those of neutral hydrogen-bonded complexes. Formation of the pnictogen bond leads to a significant increase of electron density in the bonding region between the two phosphorus atoms. One-bond spin–spin coupling constants $^1pJ(\text{P-P})$ exhibit a quadratic dependence on the P–P distance, similar to the dependence of $^2hJ(\text{X-Y})$ on the X–Y distance for complexes with X–H...Y hydrogen bonds. Thus, computed values of $^1pJ(\text{P-P})$ could be used to extract P–P distances from experimentally measured coupling constants. $^1pJ(\text{P-P})$ across the pnictogen bond arises solely from the Fermi-contact interaction, in contrast to one-bond P–P coupling constants across the covalent P–P bond in P_2H_4 which depend on PSO, FC, and SD terms.

Acknowledgments

Thanks are due to the Ohio Supercomputer Center for continuing support of this research. We also thank the Ministerio de Ciencia e Innovación (Project No. CTQ2009-13129-C02-02), the Spanish MEC (CTQ2007-62113), and the Comunidad Autónoma de Madrid (Project MADRISOLAR2, ref. S2009/PPQ-1533) for continuing support. Thanks are given to the CTI (CSIC) for an allocation of computer time.

Appendix A. Supplementary data

Supplementary data associated with this article can be found, in the online version, at [doi:10.1016/j.cplett.2011.07.043](https://doi.org/10.1016/j.cplett.2011.07.043).

References

- [1] S. Bauer, S. Tschirscowitz, P. Lönnecke, R. Franck, B. Kirchner, M.L. Clarke, E. Hey-Hawkins, *Eur. J. Inorg. Chem.* (2009) 2776.
- [2] R.D. Jackson, S. James, A. Guy Orpen, P.G. Pringle, *J. Organomet. Chem.* 458 (1993) C3.
- [3] M.R. Sundberg, R. Uggla, C. Viñas, F. Teixidor, S. Paavola, R. Kivekäs, *Inorg. Chem. Commun.* 10 (2007) 713.
- [4] S. Zahn, R. Franck, E. Hey-Hawkins, B. Kirchner, *Chem. Eur. J.* 17 (2011) 6034.
- [5] S. Tschirscowitz, P. Lönnecke, E. Hey-Hawkins, *Dalton Trans.* (2007) 1377.
- [6] J.E. Del Bene, I. Alkorta, J. Elguero, *Phys. Chem. Chem. Phys.* 13 (2011) 13951.
- [7] J.E. Del Bene, I. Alkorta, J. Elguero, *J. Phys. Chem. A*, in press, [doi:10.1021/jp203576j](https://doi.org/10.1021/jp203576j).
- [8] J.E. Del Bene, J. Elguero, in: J. Leszczynski (Ed.), *Computational Chemistry: Reviews of Current Trends*, vol. 10, World Scientific Publishing Co. Pte. Ltd., Singapore, 2006, pp. 229–264.
- [9] J.E. Del Bene, J. Elguero, I. Alkorta, *J. Phys. Chem. A* 111 (2007) 3416.
- [10] J.E. Del Bene, I. Alkorta, J. Elguero, *Magn. Reson. Chem.* 46 (2008) 457.
- [11] J.E. Del Bene, S.A. Perera, R.J. Bartlett, I. Alkorta, J. Elguero, O. Mó, M. Yáñez, *J. Phys. Chem. A* 106 (2002) 9331.
- [12] J.E. Del Bene, I. Alkorta, J. Elguero, *J. Phys. Chem. A* 114 (2010) 12958.
- [13] J.E. Del Bene, I. Alkorta, J. Elguero, *Chem. Phys. Lett.* 208 (2011) 6.
- [14] J.E. Del Bene, I. Alkorta, J. Elguero, *J. Phys. Chem. A* 113 (2009) 8359.
- [15] J.E. Del Bene, I. Alkorta, J. Elguero, *J. Phys. Chem. A* 113 (2009) 10327.
- [16] J.A. Pople, J.S. Binkley, R. Seeger, *J. Quantum Chem. Quantum Chem. Symp.* 10 (1976) 1.
- [17] R. Krishnan, J.A. Pople, *Int. J. Quantum Chem.* 14 (1978) 91.
- [18] R.J. Bartlett, D.M. Silver, *J. Chem. Phys.* 62 (1975) 3258.
- [19] R.J. Bartlett, G.D. Purvis, *Int. J. Quantum Chem.* 14 (1978) 561.
- [20] J.E. Del Bene, *J. Phys. Chem.* 97 (1993) 107.
- [21] T.H. Dunning Jr., *J. Chem. Phys.* 90 (1989) 1007.
- [22] D.E. Woon, T.H. Dunning Jr., *J. Chem. Phys.* 103 (1995) 4572.
- [23] M.J. Frisch et al., *GAUSSIAN 09*, Gaussian, Inc., Wallingford, CT, 2009.
- [24] R.F.W. Bader, in: J. Halpen, M.L.H. Green (Eds.), *Atoms in Molecules: A Quantum Theory*, The International Series of Monographs of Chemistry, Clarendon Press, Oxford, 1990.
- [25] P.L.A. Popelier, *Atoms in Molecules: An Introduction*, Prentice Hall, 2000.
- [26] AIMPAC: F.W. Bieger-Konig, R.F.W. Bader, T.H. Tang, *J. Comput. Chem.* 3 (1982) 317.
- [27] T.A. Keith, *AIMAll Program*, Version 11.04.03.
- [28] S.A. Perera, H. Sekino, R.J. Bartlett, *J. Chem. Phys.* 101 (1994) 2186.
- [29] S.A. Perera, M. Nooijen, R.J. Bartlett, *J. Chem. Phys.* 104 (1996) 3290.
- [30] A. Schäfer, H. Horn, R. Ahlrichs, *J. Chem. Phys.* 97 (1992) 2571.
- [31] J.E. Del Bene, J. Elguero, I. Alkorta, M. Yáñez, O. Mó, *J. Phys. Chem. A* 110 (2006) 9959.
- [32] S. Kirpekar, H.J.A. Jensen, J. Oddershede, *Chem. Phys.* 188 (1994) 171.
- [33] J.F. Stanton, et al., *ACES II* is a Program Product of the Quantum Theory Project, University of Florida, Integral packages included are VMOL (J. Almlof, P.R. Taylor), VPROPS (P.R. Taylor), ABACUS (T. Helgaker, H.J.A. Jensen, P. Jorgensen, J. Olsen, P.R. Taylor), Brillouin–Wigner Perturbation Theory was Implemented by J. Pittner.
- [34] I. Mata, I. Alkorta, E. Molins, E. Espinosa, *Chem. Eur. J.* 16 (2010) 2442.
- [35] J.E. Del Bene, J. Elguero, I. Alkorta, *J. Phys. Chem. A* 114 (2010) 5205.
- [36] J.E. Del Bene, J. Elguero, I. Alkorta, M. Yáñez, O. Mó, *J. Phys. Chem. A* 110 (2006) 9959.
- [37] J.E. Del Bene, J. Elguero, *J. Phys. Chem. A* 110 (2006) 12543.